Journal of Hazardous Materials 184 (2010) 499–505

Contents lists available at ScienceDirect

Journal of Hazardous Materials

journal homepage: www.elsevier.com/locate/jhazmat

Using resin supported nano zero-valent iron particles for decoloration of Acid Blue 113 azo dye solution

Hung-Yee Shu*, Ming-Chin Chang, Chi-Chun Chen, Po-En Chen

Institute of Environmental Engineering, Hungkuang University, No. 34 Chung-Chie Rd., Shalu, Taichung County 433, Taiwan, ROC

ARTICLE INFO

Article history:
Received 8 March 2010
Received in revised form 9 July 2010
Accepted 19 August 2010
Available online 26 August 2010

Keywords:
Ion exchange resin
Nano zero-valent iron
NZVI
Decoloration
Azo dye

ABSTRACT

In this study, a synthesized cation exchange resin supported nano zero-valent iron (NZVI) complex forming NZVI–resin was proposed for the decoloration of an azo dye Acid Blue 113 (AB 113), taking into account reaction time, initial dye concentration, NZVI dose and pH. From results, the successful decoloration of the AB 113 solution was observed using a NZVI–resin. Increasing the iron load to 50.8 mg g^{-1}, the removal efficiencies of the AB 113 concentration increased exponentially. With an initial dye concentration of 100 mg l^{-1} and nano iron load of 50.8 mg g^{-1}, the best removal efficiencies were obtained at 100 and 12.6% for dye concentration and total organic carbon, respectively. Color removal efficiency was dependent on initial dye concentration and iron load. Moreover, the removal rates followed modified pseudo-first order kinetic equations with respect to dye concentration. Thus, the observed removal rate constants (k) were 0.137–0.756 min^{-1} by NZVI loads of 4.9–50.8 mg g^{-1}. Consequently, the NZVI–resin performed effectively for the decoloration of AB 113 azo dye, offering great potential in the application of NZVI–resins in larger scale column tests and further field processes.

1. Introduction

In Taiwan, there are more than 250 textile dyeing and processing factories [1], making it one of the most important industries. The economic contribution of textile production is substantial, with an export revenue of 10,905 million US dollars, equal to 4.3% of the total export revenue in 2008 [2]. Nevertheless, it is difficult to decolorize effluents from textile industrials with their high color and organic concentrations. As a result, the gradual threat to the environment has attracted the attention of the public and the government. The 550 true color units of American Dye Manufactures Institute (ADMI) of the National Effluent Standard (NES) have been regulated by the Taiwan Environmental Protection Agency (TEPA) since 2003. The TEPA requires that the textile industry seek more efficient pre-treatment or polishing processes for the decoloration of high color wastewater. Moreover, azo dyes are the largest category of commercial dyes utilized in the textile industries. The di-azo dye used in this study, C.I. Acid Blue 113, is utilized extensively in various textile dyeing industries to dye wool, silk and polyamide fiber from a neutral or acid bath [3].

In this decade, innovative nanotechnology using nano scale zero-valent iron (NZVI) particles [4] have been applied in environmental treatment. Therefore, remediation has erupted promptly and dynamically. Researchers have successfully utilized NZVI and bimetallic particles for remediation of groundwater contaminated with organic chlorinated hydrocarbons such as TCE [5–7] and polychlorinated biphenyls (PCBs) [5,8] and chlorinated ethanes [9] as well as inorganics such as nitrate [10,11], perchlorate [12], and heavy metals [13–15]. In spite of successfully demonstrated in groundwater, the use of NZVI was seldom reported in the applications for wastewater treatment. Cao et al. [16] investigated the efficient decoloration of five azo dyes by ZVI under anaerobic conditions that resulted in the cleavage of azo link in the dye molecule. Nam and Trantyek [17] explored nine azo dyes with a high observed rate constant of 0.53 min^{-1} for 60 μM Crocein Orange G by ZVI of 200 g l^{-1} by ZVI followed by anaerobic biological treatment. Similarly, Mu et al. [18] obtained decoloration rate constants of 0.017 and 0.022 min^{-1} by ZVI for 0.14 and 0.71 mM of Orange II dye concentration, respectively. Using 50–200 g l^{-1} of ZVI, Chang et al. [19] presented the efficient decoloration of an Acid Black 24 (AB 24) azo dye of 100 mg l^{-1} in an ambient condition, obtaining observed pseudo-first order rate constants between 1.56 and 2.37 min^{-1}. Recently, nano particles with higher surface area and reactivity have provided a breakthrough application, that is, the use of NZVI for dye wastewater treatment. Utilizing a NZVI dose of 0.1674 g l^{-1}, a much smaller dose compared to micro-scale ZVI of 100 g l^{-1}, 100% decoloration of AB 24 has been observed. The dye removal efficiency was exponentially incremented by increasing the NZVI dosage from 0.0335 to 0.3348 g l^{-1}, obtaining the observed rate constants of 0.046–0.603 min^{-1} [20]. Lin et al. discussed the effect

* Corresponding author. Tel.: +886 4 26318652x1200; fax: +886 4 26310579.
E-mail address: hyshu@sunrise.hk.edu.tw (H.-Y. Shu).

0304-3894/$ – see front matter © 2010 Elsevier B.V. All rights reserved.
doi:10.1016/j.jhazmat.2010.08.064

of temperature on the reduction of Acid Black 24 by NZVI, obtaining an endothermic reaction of an activated energy of 72.3 kJ mol^{-1} under 10–45 °C [21]. Even though nano particles with large specific surface area and surface reactivity are superior for organic degradation, however, engineering applications of nano size have also produced new problems, such as the release or escape of nano particles into the environment resulting in nano toxicity. In addition, the process costs may increase due to the difficulty of collecting synthesized nano particles. This could result in operational difficulty in the field. Thus, immobilizing NZVI particles on supporting materials does not only provide an easy operation but also maintains the excellent reduction ability of NZVI. In another study, ion exchange resin was efficiently utilized for adsorbing heavy metals in industrial wastewater which could be used as carriers of catalysts, such that, ferric ion immobilized resin was conducted to perform an effective Fenton-like reaction for the degradation of phenol and salicylic acid [22,23]. The dechlorination of trichloroethylene by immobilized ZVI on a cationic exchange membrane was successfully demonstrated by Kim et al. [24]. Moreover, Li et al. [25] employed innovative immobilizing NZVI nano particles with resin in the effectual debromination of brominated diphenyl ether. Thus, cation exchange resin has been proven to be an excellent carrier for metal ions and nano particles.

The purpose of this study was to examine the feasibility of the degradation of Acid Blue 113 using the NZVI–resin, evaluating time, NZVI load, initial dye concentration, and pH. In addition, the modified pseudo-first order kinetic equation and removal efficiency as function of the NZVI load was developed for the calculation of kinetic rate constants.

2. Materials and methods

2.1. Materials

The chemical structure of the dye C.I. Acid Blue 113 (C.I. 26360, $C_{32}H_{21}N_5Na_2O_6S_2$, molecular weight 681.7, characteristic wavelength 566 nm, AB 113) is shown in Fig. 1a. The dye was obtained from Sigma–Aldrich, Inc., with no further purification for use. Commercially available Dowex HCR-W2 cation resin was purchased from Sigma–Aldrich Inc. for preparing the resin with nano zero-valent iron complex (NZVI–resin). Chemicals in reagent grade such as iron chloride ($FeCl_3$) and sodium borohydride ($NaBH_4$) were both purchased from Merck & Co., Inc.

The NZVI–resin complex was prepared by initially weighing 20.0 g of HCR-W2 cation exchange resin and storing it in a 250 ml width-mouth plastic bottle. The resin was mixed with 200 ml of iron chloride solution and shaken at 100 rpm for 4 h to homogeneously obtain ferric iron (Fe^{3+}) absorption in the resin. The ferric iron concentration distribution in the resin was calculated by initial concentration to deduct the residual iron in the $FeCl_3$ solution from the supernatant drawn to be analyzed by a SHIMADZU AA-6200 Atomic Absorption Spectroscopy. Moreover, the resin was washed by de-ionized (DI) water three times to remove residual $FeCl_3$ solution. Later, 0.8 M of $NaBH_4$ solution was added to obtain NZVI precipitation in the resin at an ambient temperature following Eqs. (1) and (2). The above method was modified from a previous study [20]. Afterwards, DI water was used to wash the NZVI–resin three times and remove residual $NaBH_4$ solution. A partial amount of the NZVI–resin was taken to identify the morphology by a JEOL 6330CF Field Emission Scanning Electron Microscope (FESEM). The morphology image of NZVI free resin is shown in Fig. 1b and the NZVI–resin shown in Fig. 1c and d. In this way, the particle sizes of the NZVI–resin within 40–170 nm were calculated by numerical treatment of FESEM image. A Micromeritics Gemini V Automated Gas Sorption System was employed to identify the NZVI–resin BET

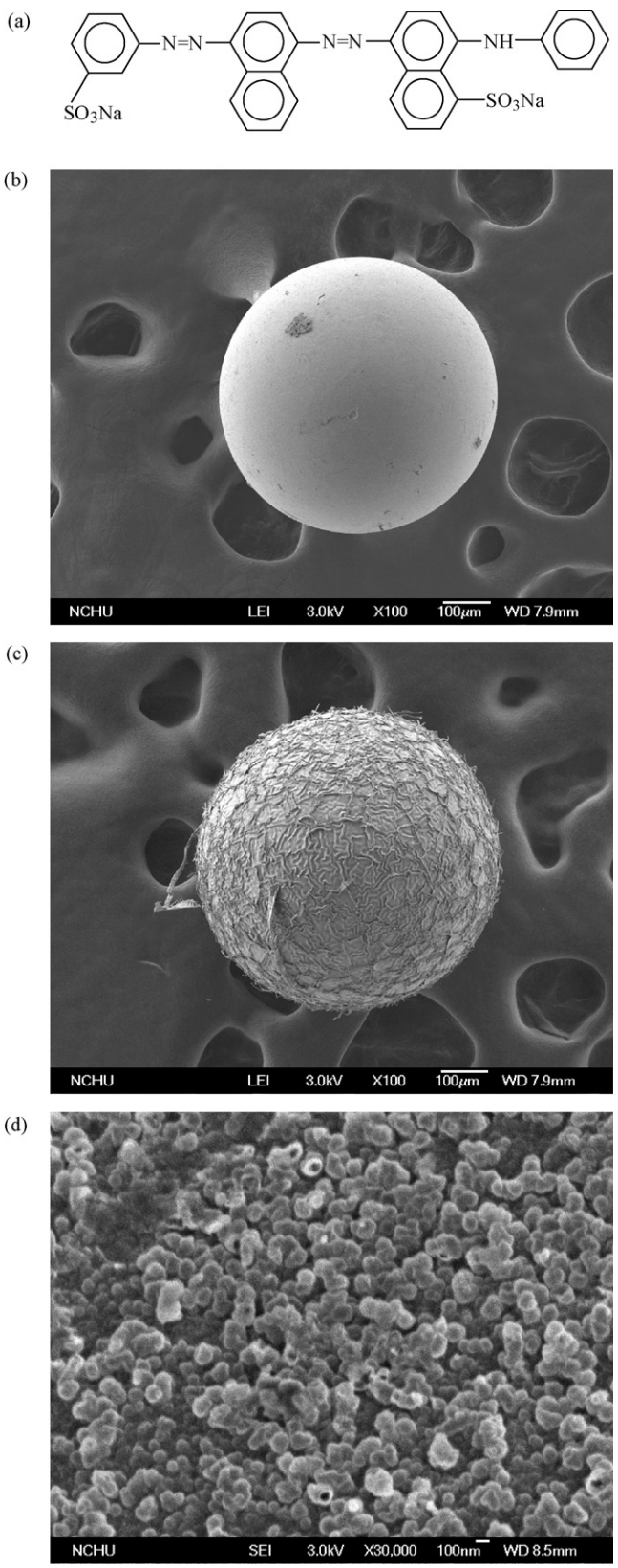

Fig. 1. (a) Structure of C.I. Acid Black 113, and morphology of (b) resin ×100, (c) resin supported nanoscale zero-valent iron complex material (NZVI–resin) ×100, and (d) NZVI–resin ×30,000 by a JEOL 6330CF Field Emission Scanning Electron Microscope (FESEM).

(Brunauer, Emmett, and Teller) surface area of 1.298 $m^2\,g^{-1}$. There is only 50 mg g^{-1} of NZVI loaded in the NZVI–resin. This could be calculated to obtain a BET surface area of 25.96 $m^2\,g^{-1}$ based on bare NZVI without resin.

$$2Fe(H_2O)_6^{3+} + 6BH_4^- + 6H_2O \rightarrow 2Fe^0 \downarrow + 6B(OH)_3 + 21H_2 \quad (1)$$

$$2[Fe^{3+}\text{-}(resin)^{3-}] + 6NaBH_4 + 18H_2O \rightarrow 2Fe^0/6Na^+\text{-}(resin)^{6-} \downarrow + 6B(OH)_3 + 21H_2 \quad (2)$$

2.2. Experimental procedure

The amount (in mg unit) of dye AB 113 was precisely measured to dissolve into 1 l of DI water, obtaining a concentration of mg l^{-1} unit. The NZVI–resin was initially prepared by 20 g resin in a 200 ml iron chloride solution of 8.95, 17.9, 35.8, 53.7, 71.6 and 107.4 mM to obtain loadings of 50, 40, 30, 20, 10 and 5 mg NZVI per g resin. 20 g of NZVI–resin was placed in the 1-l batch reactor. The AB 113 dye solution was poured into the reactor, taking into consideration the time, loading of NZVI on NZVI–resin, initial dye concentration, and pH at mixing rate of 300 rpm. At defined time intervals, the dye concentration in water samples were withdrawn and measured by a Hitachi U-2000 spectrophotometer with single wavelength absorbance (572 nm). Several sets of calibration curves were prepared under various pH conditions (i.e. pH 2, 3, 6, 9 and 12) to reflect the variation of characteristic wavelength and absorbance. And these calibration curves were used to measure the AB 113 concentrations under various pH conditions to avoid expected error. The total organic carbon (TOC) was also determined by an IO Analytical 1030W Total Organic Carbon analyzer. The standard color detection procedure developed by the American Dye Manufacturers Institute (ADMI) was employed to evaluate the color intensity of AB 113 dye solution. The color intensity was calculated by applying the Adams–Nickerson color difference formula, which substituted transmittance data obtained into 30 wavelengths from 400 to 700 nm in every 10 nm interval, following method 2120E of the Standard Methods [26]. The pH and ORP were monitored by a Eutech PH5500 dual channel pH/ion meter with specific probes. The iron concentration was measured by a Shimadzu AA-6200 Atomic Absorption Spectrophotometer.

3. Results and discussion

3.1. Effects of reaction time and initial dye concentration

As shown in previous studies, the dissolution of ferrous ions and electrons to react with organic molecules on the iron surface and reduction by zero-valent iron in the aqueous phase has been proven to be a fairly fast process [20]. The performance of NZVI–resin follows a mechanism similar to iron dissolution, with the re-capture of free ferrous ions on the resin surface to avoid total iron release. Fig. 2 shows the effect of reaction time on the degradation of AB 113 dye with the addition of 20 g l^{-1} of 50.8 mg g^{-1} loaded NZVI–resin and five initial dye concentrations. Within the first 2 min, the removal of dye concentration was about 50–70%, increasing sharply up to10 min. There was barely any change after 10 min. The AB 113 dye concentration quickly dropped down to 6.1 mg l^{-1} and achieved 93.9% removal efficiency during 10 min with the initial concentration of 100 mg l^{-1}. Moreover, no significant change was found until 60 min. This scenario implies that the reductive degradation of AB 113 occurs initially within the first 10 min. Afterwards, the AB 113 concentration removal rarely changes. Moreover, the initial dye concentration increased from 50 to 600 mg l^{-1}, resulting in the increase of the residual dye concentration. From the results, pH increased sharply from 5.6 to 8.0 in 4 min and then decreased smoothly to 6.8 at the end, as shown in Fig. 3a. The explanation of pH change in first 4 min is according to the mechanism of NZVI dissolution, spontaneously the hydroxyl ions are released into the solution and causes the increase of pH from 5.6 to 8.0. After all, the formation and deposition of ferrous hydroxide on resin surface makes the pH decrease to 6.8. For the initial dye concentration of 100 mg l^{-1}, the oxidation reduction potential (ORP) dropped from 322.3 to −641.6 mV as soon as the NZVI–resin was added. The ORP remained at about −600 mV in the first 10 min, later turning sharply to −178.4 mV at the end of reaction time (60 min). This shows that the typical reductive condition of the AB 113 dye solution was reduced within the first 10 min. After 15 min, little effective dye degradation can be found. Simultaneously, the ADMI color index decreased sharply from 30956 down to less than 3339 in 4 min, rebounding to 9798 units in 15 min, as shown in Fig. 3b. The rebound was due to the formation of ferric ions. In the end, the color index decreased to less than 2000 ADMI.

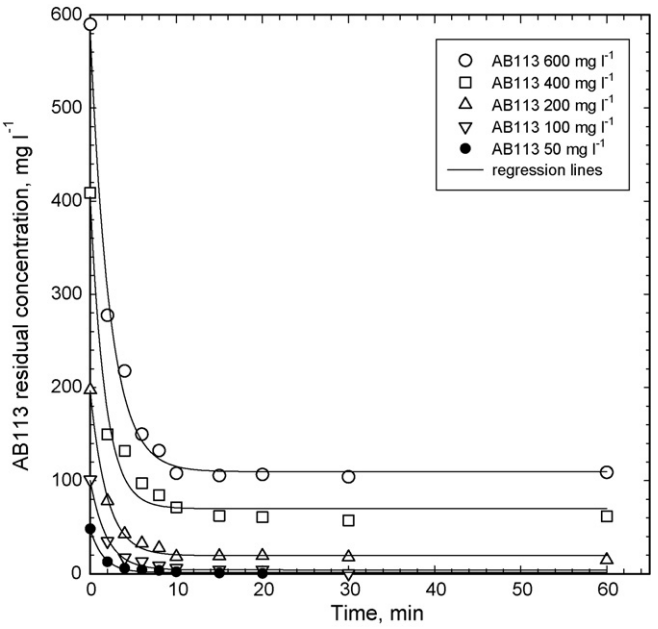

Fig. 2. AB 113 residual concentration versus time for NZVI–resin reduction degradation of 50–600 mg l^{-1} initial dye concentration, 20 g l^{-1} NZVI–resin addition with 50 mg g^{-1} load of NZVI and 100 rpm of mixing speed.

Fig. 4 summarizes the effect of the initial dye concentration on dye degradation efficiency and the amount of dye degraded per unit weight of NZVI (unit NZVI AB 113 removal capacity). The maximum removal efficiency (Rmax) declined from 100 to 80.4% when initial dye concentration increased from 50 to 600 mg l^{-1}. The initial rate (r_0) used to evaluate the effect of the initial dye concentration increased from 17.64 to 33.01 and 156.15 mg l^{-1} min^{-1}, with initial AB 113 concentration increasing from 50 to 100 and 600 mg l^{-1}, respectively. The figure shows that the unit NZVI AB 113 removal capacity (URC) is the function of the initial AB 113 concentration (50–600 mg l^{-1}). Over the course of 60 min, the URCs were 0.047, 0.097, 0.339 and 0.480 mg AB 113 per mg NZVI with initial dye concentrations of 50, 100, 400 and 600 mg l^{-1} by the addition of 20 g l^{-1} of 50.8 mg g^{-1} loaded NZVI–resin. However, higher initial concentrations of AB 113 obtained lower dye degradation efficiencies, which provided higher unit NZVI AB 113 removal capacities at the same resin and NZVI dosage. Thus, higher initial dye AB 113 concentration showed higher unit NZVI AB 113 removal capacity.

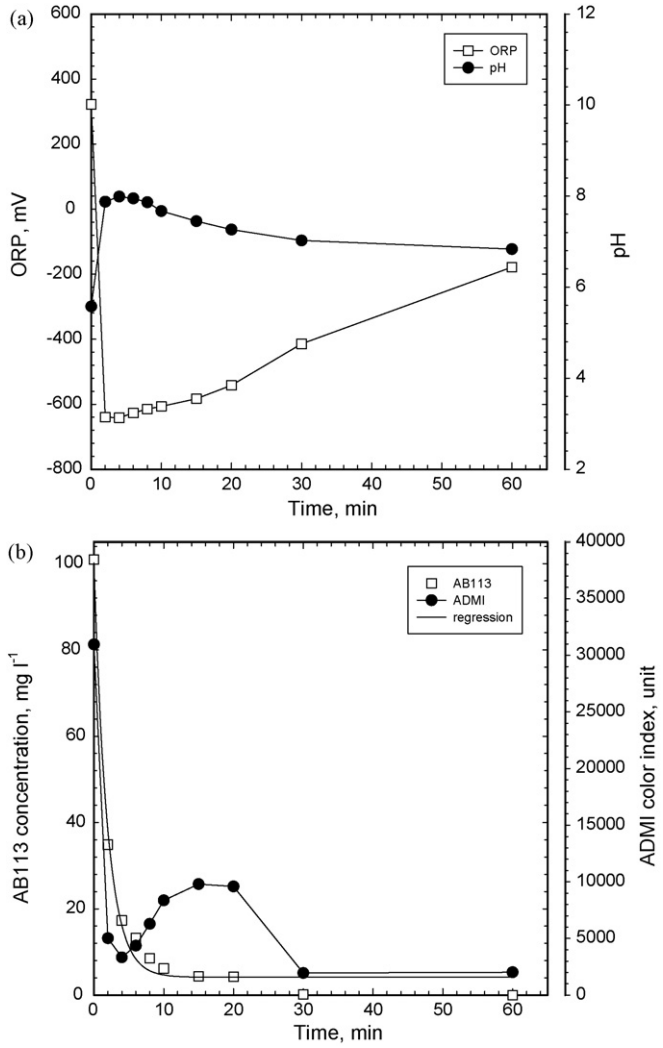

Fig. 3. (a) pH and ORP and (b) AB 113 and ADMI color index for NZVI–resin reduction degradation of 100 mg l^{-1} AB 113 with 20 g l^{-1} NZVI–resin addition, 50 mg g^{-1} load of NZVI and 100 rpm of mixing speed.

Degradation of AB 113 certainly occurs on the NZVI surface. The surface is gradually occupied by dissolved oxygen and oxidative species from the reactions resulting in the loss of reactivity. Thus, excessively stoichiometric amounts of NZVI loads on the resin were employed to avoid variation of NZVI concentration by corrosion during reaction. Colored dye concentration degradation is generally

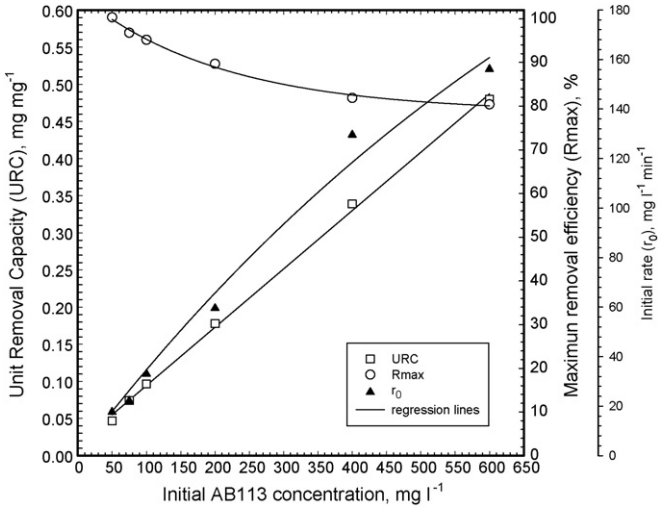

Fig. 4. The relationships between unit removal capacity (URC), maximum removal efficiency (Rmax) and initial rate (r_0) versus initial AB 113 concentration. The operating conditions were same as Fig. 2.

assumed to be a first-order reaction with respect to dye concentration, ignoring NZVI concentration. It converts to a pseudo-first order reaction (Eq. (3)).

$$C_{dye} = C_{dye0} \times e^{-kt} \quad (3)$$

where k denotes the observed first-order reaction rate constant, t the reaction time, C_{dye0} the initial concentration of AB 113, and C_{dye} is the concentration of AB 113 at time t. When the reaction occurs in water/NZVI interphase, this limits phase transfer, making it difficult to reach 100% degradation efficiency. Thus, the residual dye concentration is modified as Eq. (4).

$$C_{dye} = C_{ultimate} + (C_{dye0} - C_{ultimate}) \times \alpha \times e^{-kt} \quad (4)$$

where $C_{ultimate}$ is the ultimate residual AB 113 concentration for the NZVI reduction process, α is the variation coefficient to the ideal first-order kinetic (1.0 denotes ideal first-order kinetic, the larger the deviation from 1.0, the less fit the first-order kinetics). $C_{ultimate}$, α and k can be obtained by non-linear regression from Fig. 2. Thus, higher initial dye concentrations produced significantly higher ultimate residual dye concentrations. The ultimate residual AB 113 concentrations, $C_{ultimate}$ of 1.35 and 109.62 mg l^{-1} and first-order rate constants, k of 0.648 and 0.443 min^{-1} were obtained with the initial dye concentrations of 50 and 600 mg l^{-1}, respectively. The first-order rate constants were in the same order of magnitude when compared with the results of Nam and Trantyek [17]. They presented a higher observed rate constant of 0.530 min^{-1}

Table 1
Results of the non-linear regression of experimental data by Eq. (4).

Initial pH	C_{dye0} (mg l^{-1})	NZVI load (mg g^{-1})	$C_{ultimate}$	α	k (min^{-1})	R^2
5.6	50	50.8	1.35	0.959	0.648	0.991
5.6	75	50.8	0.097	0.995	0.480	0.998
5.6	100	50.8	4.14	1.002	0.519	0.991
5.6	200	50.8	19.54	0.980	0.521	0.996
5.6	400	50.8	69.94	1.014	0.582	0.978
5.6	600	50.8	109.62	0.967	0.443	0.991
5.6	100	4.9	88.14	0.996	0.756	0.951
5.6	100	9.9	53.52	0.946	0.137	0.986
5.6	100	19.9	21.82	0.996	0.208	0.998
5.6	100	29.8	12.16	1.012	0.248	0.998
5.6	100	37.7	6.45	0.995	0.591	0.995
2	100	29.8	72.61	0.991	0.639	0.973
3	100	29.8	60.57	1.038	0.419	0.943
9	100	29.8	10.98	0.985	0.442	0.985
12	100	29.8	78.84	0.968	0.261	0.982

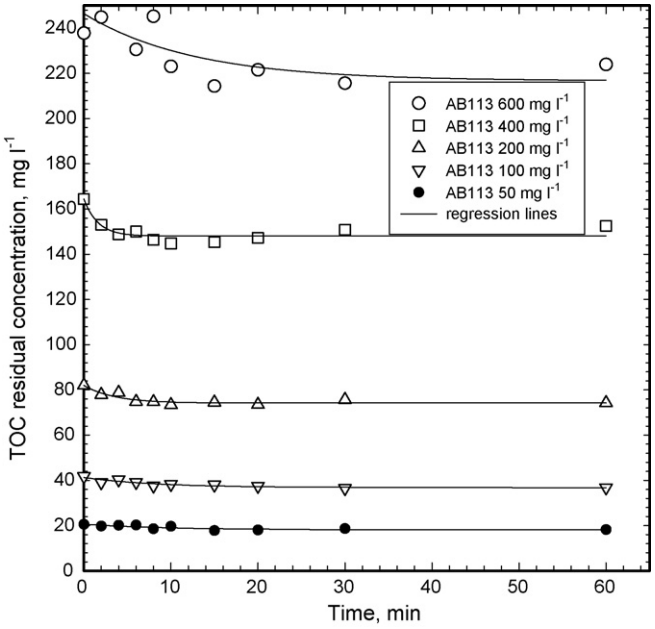

Fig. 5. Residual TOC concentration versus time for NZVI–resin reduction degradation of AB 113 dye, the operating conditions were same as Fig. 2.

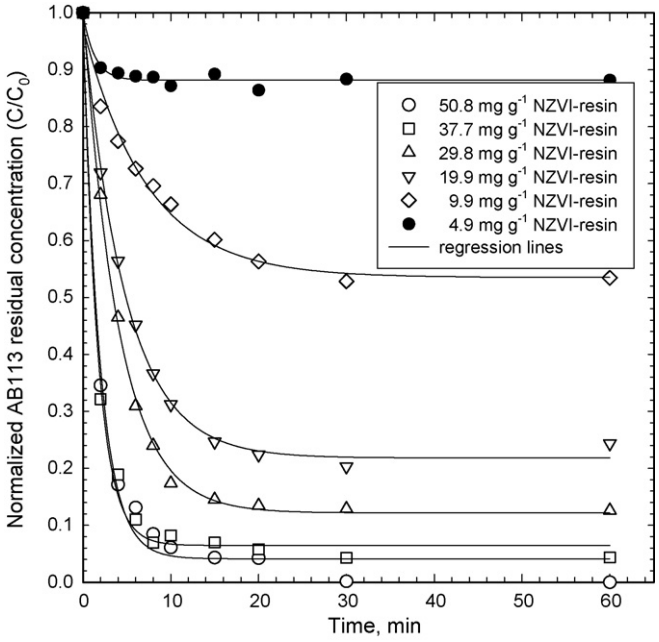

Fig. 6. Normalized AB 113 concentration versus time for NZVI–resin reduction degradation of 100 mg l^{-1} initial dye concentration with various NZVI–resin loads.

and a lower rate constant of 0.023 min^{-1} in the decoloration of 60 μM Crocein Orange G and 300 μM Naphthol Blue Black G adding 200 g l^{-1} iron, respectively. The 1.0 g l^{-1} iron of NZVI–resin used in this study is much lower than the 200 g l^{-1} of micro-scale iron mentioned above. Similarly, Mu et al. reported rate constants between 0.017 and 0.022 min^{-1} for 0.14–0.71 mM Orange II decolorized by 66.6 g l^{-1} iron [18]. This implies the greater surface area of the NZVI–resin in this study demonstrated improved decoloration. The regression parameters and R^2 in Eq. (4) are summarized in Table 1.

Fig. 5 presents the effect of TOC removal versus reaction time for five various initial dye concentrations. The results show that the TOC reduction of the AB 113 solution was more difficult to reach than 100% dye degradation efficiency. A maximum of 12.6% TOC removal efficiency was reached with the initial dye concentration of 100 mg l^{-1}. TOC concentrations were slightly and exponentially decreased during the reductive decoloration so that TOC removal efficiencies were less than 15%, regardless of the initial dye concentration. A previous study presented the effective decoloration of an azo dye, Orange II, to cleave azo link forming products such as sulfanilic acid and 1-amino-2naphthol [18]. Similarly, in this study, the degradation of AB 113 by NZVI–resin produced smaller molecular size fragments of sulfanilic acid and aromatic amines. This contributed to TOC concentration. During the reaction, a small portion of TOC was reduced by adsorption on NZVI–resin, but the major part of the TOC remained in the solution. In a NZVI process, the reason for TOC removal by NZVI reduction was extremely limited by the adsorption surface, so that adding certain dosage of NZVI can effectively break the chromophore (i.e. azo links) of azo dye and decolorize the solution but only achieve limited TOC removal. It is very important to solve an environmental problem by removing and converting pollutants to their nontoxic form. Thus, integrating an oxidative process to combine with NZVI–resin process may provide a total decolorization and mineralization solution of azo dye treatment. This idea can be presented from our previous work, a C.I. Acid Black 24 synthesized wastewater was successfully removed synchronously its total color and total organic carbon (TOC) using an integrated innovation technology by coupling the zero-valent iron (ZVI) nanoparticles with UV/H_2O_2 oxidation process [27].

3.2. Effect of the NZVI load on the resin

The effect of the NZVI load on the resin shown in Fig. 6 indicates that AB 113 degradation efficiency increased with the increase of the NZVI load. Thus, the residual dye concentration is the function of the NZVI load and reaction time by 4.9–50.8 mg g^{-1} NZVI–resin with an initial AB 113 concentration of 100 mg l^{-1}. Increasing the load of NZVI on the resin provided substantially more active surface sites to accelerate the initial reaction, resulting in more NZVI surface collision with more azo dye molecules to enhance AB 113 degradation. From the experimental data, the degradation efficiencies of 11.8, 75.6 and 100% were obtained by the NZVI loads of 4.9, 19.9, and 50.8 mg g^{-1} over 60 min, respectively. Moreover, the degradation efficiencies of AB 113 were found to be dependent on the NZVI load, as shown in Fig. 7. It is shown that with greater NZVI loads on the resin the number of reactive NZVI sites increased

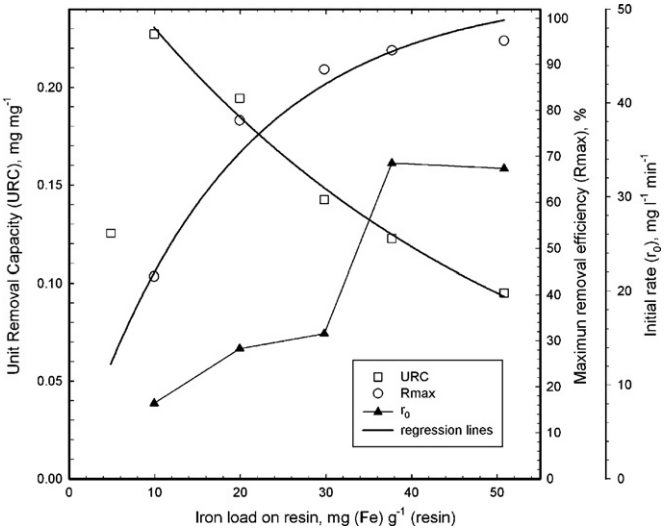

Fig. 7. The relationships between unit removal capacity (URC), maximum removal efficiency (Rmax) and initial rate (r_0) versus NZVI–resin loads.

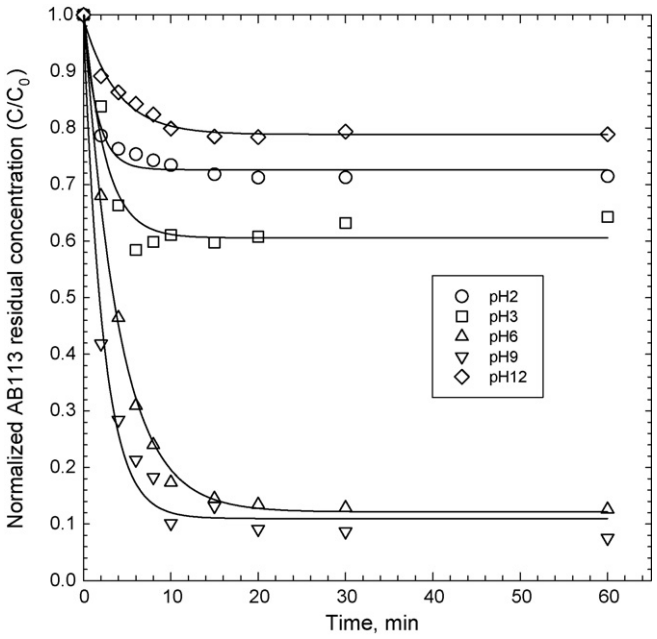

Fig. 8. Normalized AB 113 residual concentration versus time for NZVI–resin reduction degradation of 100 mg l^{-1} initial dye concentration under various pH. The operating conditions were same as Fig. 2.

proportionally. As a result, dye degradation efficiency increased exponentially up to a NZVI load of 37.7 mg g^{-1}. Thus, a first-order expression was derived by non-linear regression as follows,

$$R(\%) = 106.01 \times (1 - e^{-0.0553 \times D}) \quad (5)$$

where $R(\%)$ is the dye removal efficiency in % for a certain NZVI load, and D expresses the NZVI load in units of mg g^{-1}.

The effect of NZVI load on dye degradation amounts per unit weight of NZVI is also summarized in Fig. 7. It is apparent that the unit NZVI dye removal capacities (URCs) are the function of NZVI load (4.9–50.8 mg g^{-1}). The URCs are 0.227, 0.194 and 0.095 mg AB 113/mg NZVI by NZVI loads of 9.9, 29.9, and 50.8 mg g^{-1} for initial dye concentration of 100 mg l^{-1} over the course of 60 min. The higher NZVI loads obtained higher dye removal; nevertheless, they provided lower URCs at the same initial dye concentration. Thus, an exponential decay expression was derived as follows for NZVI loads from 9.9 to 50.8 mg g^{-1},

$$\text{URC}(\text{mg AB113/mg NZVI}) = 0.287 \times e^{-0.022 \times D} \quad (6)$$

where URC is the amount of dye degraded per unit weight of NZVI for certain NZVI loads, and D is the NZVI load in units of mg g^{-1}.

The lowest URC at the NZVI load of 4.9 mg g^{-1} did not follow Eq. (6). This is because it is difficult for low NZVI loads to fully react with the dye. This could result from the competition of reactive sites of AB 113 with dissolved oxygen and inorganic species. The initial degradation rate of AB 113, r_0, increased with the increase of NZVI loads, as shown in Fig. 7. This was calculated by deducing the dye concentration during the first 2 min over time. From the experimental data, the initial rates of 4.72, 13.89 and 33.01 mg l^{-1} min^{-1} were obtained by the NZVI loads of 4.9, 19.9, and 50.8 mg g^{-1}, respectively.

3.3. Effect of pH

Fe^{2+} ions from the iron surface and hydroxyl ions in the alkaline solution reacted to precipitate ferrous hydroxide on the surface of the iron occupying the reactive sites, thus hindering the reaction. Thus, by raising pH to the alkaline region Shu et al. observed lower decolorization rates under NZVI reduction conditions were by [20]. The effect of pH in the degradation of AB 113 by NZVI–resin is illustrated in Fig. 8 with initial dye concentration of 100 mg l^{-1} and NZVI load of 29.8 mg g^{-1}. Elevating the pH to 12 by addition of sodium hydroxide solution (1.0 mol l^{-1}) resulted in significant reduction of dye degradation efficiency, whereas reducing the pH to 2 by the addition of hydrochloric acid (1.0 mol l^{-1}) also resulted in the extreme decrease of dye degradation efficiency by more than 58% compared with the original pH. This implies that extreme pH levels such as 2 and 12 inhibit degradation of AB 113 for different reasons. For an alkaline pH of 12, the precipitation of ferrous hydroxide on the surface of the NZVI occupying the reactive sites stopped the release of ferrous ions and electrons that cause the lowering of the reaction rate. For an acidic pH of 2, the NZVI dissolved quickly into the bulk solution, resulting in an insufficient amount of surface area for the release of ferrous ions and electrons that degrade dye. For middle pH levels from 6 to 9, degradation of AB 113 was performed fairly efficiently with no significant differences.

4. Conclusions

We have shown that reductive degradation of AB 113 di-azo dye in aqueous solution can be achieved in less than 20 min by adding resin supported nano zero-valent iron complex material, namely NZVI–resin, under ambient conditions without pH control. After 30 min, almost 100% AB 113 concentration and 12.6% TOC removal were reached with a 50.8 mg g^{-1} NZVI load and a 20 g l^{-1} resin and initial dye solution of 100 mg l^{-1}. In our batch test, the kinetics of the AB 113 reduction was dominated by the NZVI load as well as the initial dye concentration and pH. The kinetics of AB 113 reduction was developed as a modified pseudo-first order reaction with respect to the AB 113 concentration in the presence of the stoichiometric excess of NZVI surface. As a result, the observed reaction rate constants were 0.137–0.756 min^{-1} for NZVI loads of 4.9–50.8 mg g^{-1}. Furthermore, the degradation efficiency exponentially increased with increased NZVI load. Accordingly, the results of this study on the effects of NZVI loads, initial dye concentration and pH can optimize the operating parameters of AB 113 degradation and provide industries with useful information about this alternative wastewater technology.

Acknowledgement

The authors appreciate the research funding granted by the Taiwan National Science Council (NSC 96-2221-E-241-005-MY2).

References

[1] C.M. Kao, M.S. Chou, B.W. Fang, B.R. Huang, Regulating colored textile wastewater by 3/31 wavelength admi methods in Taiwan, Chemosphere 44 (2001) 1055–1063.
[2] Taiwan Ministry of Finance, Brief Export-Import Statistics Monthly (Air Mail Edition)/Summary Explanation for December 2008 (Department of Statistics – 2009/2/23); http://www.mof.gov.tw/engweb/ct.asp?xItem=28631&CtNode=683&mp=2 (accessed 10.08.09).
[3] F.J. Green, The Sigma–Aldrich Handbook of Stains, Dyes and Indicators, second ed., Aldrich Chemical Company, Inc., Wisconsin, 1991.
[4] T. Masciangioli, W.X. Zhang, Environmental technologies at the nanoscale, Environ. Sci. Technol. 37 (2003) 102A–108A.
[5] C.B. Wang, W.X. Zhang, Synthesizing nanoscale iron particles for rapid and complete dechlorination of TCE and PCBs, Environ. Sci. Technol. 31 (1997) 2154–2156.
[6] Y.Q. Liu, G.V. Lowry, Effect of particle age (Fe-o content) and solution pH on NZVI reactivity: H-2 evolution and TCE dechlorination, Environ. Sci. Technol. 40 (2006) 6085–6090.
[7] Y.Q. Liu, S.A. Majetich, R.D. Tilton, D.S. Sholl, G.V. Lowry, TCE dechlorination rates, pathways, and efficiency of nanoscale iron particles with different properties, Environ. Sci. Technol. 39 (2005) 1338–1345.
[8] G.V. Lowry, K.M. Johnson, Congener-specific dechlorination of dissolved PCBs by microscale and nanoscale zerovalent iron in a water/methanol solution, Environ. Sci. Technol. 38 (2004) 5208–5216.

[9] H.L. Lien, W.X. Zhang, Hydrodechlorination of chlorinated ethanes by nanoscale Pd/Fe bimetallic particles, J. Environ. Eng. ASCE 131 (2005) 4–10.
[10] K. Sohn, S.W. Kang, S. Ahn, M. Woo, S.K. Yang, Fe(0) nanoparticles for nitrate reduction: stability, reactivity, and transformation, Environ. Sci. Technol. 40 (2006) 5514–5519.
[11] Z. Xiong, D.Y. Zhao, G. Pan, Rapid and controlled transformation of nitrate in water and brine by stabilized iron nanoparticles, J. Nanopart. Res. 11 (2009) 807–819.
[12] Z. Xiong, D.Y. Zhao, G. Pan, Rapid and complete destruction of perchlorate in water and ion-exchange brine using stabilized zero-valent iron nanoparticles, Water Res. 41 (2007) 3497–3505.
[13] C. Uzum, T. Shahwan, A.E. Eroglu, K.R. Hallam, T.B. Scott, I. Lieberwirth, Synthesis and characterization of kaolinite-supported zero-valent iron nanoparticles and their application for the removal of aqueous Cu2+ and Co2+ ions, Appl. Clay Sci. 43 (2009) 172–181.
[14] B. Geng, Z.H. Jin, T.L. Li, X.H. Qi, Kinetics of hexavalent chromium removal from water by chitosan-Fe-0 nanoparticles, Chemosphere 75 (2009) 825–830.
[15] S.Y. Chen, W.H. Chen, C.J. Shih, Heavy metal removal from wastewater using zero-valent iron nanoparticles, Water Sci. Technol. 58 (2008) 1947–1954.
[16] J. Cao, L. Wei, Q. Hunag, L. Wang, S. Han, Reductive degradation of azo dye by zero-valent iron in aqueous solution, Chemosphere 38 (1999) 565–571.
[17] S. Nam, P.G. Trantyek, Reduction of azo dyes with zero-valent iron, Water Res. 34 (2000) 1837–1845.
[18] Y. Mu, H.Q. Yu, S.J. Zhang, J.C. Zheng, Kinetics of reductive degradation of orange II in aqueous solution by zero-valent iron, J. Chem. Technol. Biotechnol. 79 (2004) 1429–1431.
[19] M.C. Chang, H.Y. Shu, H.H. Yu, Y.C. Sung, Reductive decolorization and TOC reduction of the di-azo dye C.I. Acid Black 24 by zero-valent iron powder, J. Chem. Technol. Biotechnol. 81 (2006) 1259–1266.
[20] H.Y. Shu, M.C. Chang, H.H. Yu, W.H. Chen, Removal of di-azo dye Acid Black 24 in synthesized wastewater using zero-valent iron nanoparticle, J. Colloid Interface Sci. 314 (2007) 89–97.
[21] Y.T. Lin, C.H. Weng, F.Y. Chen, Effective removal of AB24 dye by nano/micro-size zero-valent iron, Sep. Purif. Technol. 64 (2008) 26–30.
[22] R.M. Liou, S.H. Chen, M.Y. Hung, C.S. Hsu, J.Y. Lai, Fe (III) supported on resin as effective catalyst for the heterogeneous oxidation of phenol in aqueous solution, Chemosphere 59 (2005) 117–125.
[23] J. Feng, X. Hu, P.L. Yue, Degradation of salicylic acid by photo-assisted Fenton reaction using Fe ions on strongly acidic ion exchange resin as catalyst, Chem. Eng. J. 100 (2004) 159–165.
[24] H. Kim, H.J. Hong, Y.J. Lee, H.J. Shin, J.W. Yang, Degradation of trichloroethylene by zero-valent iron immobilized in cationic exchange membrane, Desalination 223 (2008) 212–220.
[25] A. Li, C. Tai, Z.S. Zhao, Y.W. Wang, Q.H. Zhang, G.B. Jiang, J.T. Hu, Debromination of decabrominated diphenyl ether by resin-bound iron nanoparticles, Environ. Sci. Technol. 41 (2007) 6841–6846.
[26] APHA, AWWA, WPCF, Standard Methods for the Examination of Water and Wastewater, ninth ed., American Public Health Association, Washington, DC, 1995.
[27] H.Y. Shu, M.C. Chang, C.C. Chang, Integration of nanosized zero-valent iron particles addition with UV/H_2O_2 process for purification of azo dye Acid Black 24 solution, J. Hazard. Mater. 167 (2009) 1178–1184.